Journal of Chromatography B, 879 (2011) 1105–1111

Contents lists available at ScienceDirect

Journal of Chromatography B

journal homepage: www.elsevier.com/locate/chromb

Strategies for the purification and characterization of protein scaffolds for the production of hybrid nanobiomaterials

Germán Plascencia-Villa, Jimmy A. Mena [1], Ricardo M. Castro-Acosta, Julio César Fabián, Octavio T. Ramírez, Laura A. Palomares *

Departamento de Medicina Molecular y Bioprocesos, Instituto de Biotecnología, Universidad Nacional Autónoma de México, A.P. 510-3, C.P. 62210, Cuernavaca, Morelos, Mexico

ARTICLE INFO

Article history:
Received 28 September 2010
Accepted 13 March 2011
Available online 21 March 2011

Keywords:
Rotavirus
Nanobiomaterials
Chromatography
Multimeric proteins
Baculovirus

ABSTRACT

Rotavirus VP6 self-assembles into high order macrostructures useful as novel scaffolds for the construction of multifunctional hybrid nanobiomaterials. This application requires large quantities of high quality pure material with strict structural consistency. Strategies for obtaining high quality recombinant VP6 and different characterization techniques are explored and compared in this work. VP6 was expressed in the insect cell–baculovirus system. VP6 assemblies were selectively purified utilizing an ion exchange and size exclusion (SE) chromatography. Purification steps were monitored and characterized by dynamic light scattering (DLS), ELISA, SDS-PAGE, HPLC and Western blot. DLS showed that the initial ultrafiltration step removed small particles, the intermediate anion exchange chromatographic step completely removed the baculovirus, whereas the final size exclusion chromatography permitted the selective recovery of correctly assembled VP6 nanotubes and discrimination of non-assembled VP6, as confirmed by transmission electron microscopy. VP6 assembled into tubular structures with diameter of 75 nm and several nanometers in length. The purification yield was 20% of multimeric assemblies with a purity >98%. The resulting material was suitable for the production of functionalized hybrid nanobiomaterials through *in situ* synthesis of metallic nanoparticles.

1. Introduction

Protein nanotubes are highly ordered self-assembled macrostructures. These multimeric arrays are functional building blocks that can direct the interaction and specific location of different functional materials and biomolecules for the fabrication of hybrid materials [1]. Protein nanotubes have a stable biocompatible structure with molecular recognition abilities and can be functionalized through bioconjugation for applications in nanomedicine, diagnostics, drug delivery, material sciences, bioelectronics, nano-composites and catalysis [1–4]. Biological materials display remarkable unique properties that are difficult to obtain even with advanced synthetic technologies, such as carbon or inorganic nanotubes.

Protein nanotubes have been obtained from various sources, such as protein filaments, microtubules, collagen, amyloid fibers, bacterial pili and flagella, engineered peptides and complete helical viruses [1,3,5–7]. Less explored as nanobiomaterials are recombinant viral capsid proteins with self-assembly capacity. An example is rotavirus VP6, which is the major component of the icosahedral rotavirus capsid and can self-assemble into nanotubes or icosahedra depending on pH, ionic strength, divalent ion and protein concentrations [8,9]. VP6 nanotubes are hollow, homogeneous, highly organized, symmetric and robust structures that can be used as multifunctional building blocks for the construction of highly organized, integrative and functional nanobiomaterials [10]. The structural characteristics of VP6 and its intrinsic high affinity for metal ions have allowed its use as a multifunctional molecular scaffold for the synthesis of novel integrated hybrid nanobiomaterials functionalized by the *in situ* conjugation of silver, gold, platinum and palladium nanoparticles [10].

The use of recombinant viral capsid proteins as nanobiomaterials has several advantages, as fewer safety concerns exist in comparison with the synthesis of nanomaterials derived from live virus. In addition, their production is less expensive and environ-

Abbreviations: AEX, anion-exchange chromatograpy; bacVP6, baculovirus coding for rotavirus VP6 strain SA11; DLS, dynamic light scattering; ELISA, enzyme-linked immunoassay; IC–BEVS, insect cell–baculovirus expression vector system; MOI, multiplicity of infection; pfu, plaque forming unit; SE, size exclusion; TEM, transmission electron microscopy.

* Corresponding author. Tel.: +52 777 329 1863; fax: +52 777 313 8811.
E-mail addresses: germanpv@ibt.unam.mx (G. Plascencia-Villa), yimy.mena@cnrc-nrc.gc.c (J.A. Mena), rcastro@ibt.unam.mx (R.M. Castro-Acosta), faga170777@yahoo.com.mx (J.C. Fabián), tonatiuh@ibt.unam.mx (O.T. Ramírez), laura@ibt.unam.mx (L.A. Palomares).
[1] Present address: Animal Cell Technology Group, Biotechnology Research Institute, National Research Council Canada. Montreal, Quebec, Canada.

1570-0232/$ – see front matter © 2011 Elsevier B.V. All rights reserved.
doi:10.1016/j.jchromb.2011.03.027

mentally friendly [2,4]. However, the production and purification of such highly ordered protein structures have their own challenges. In contrast to the production of monomeric recombinant proteins, assuring a high concentration of recombinant protein is not enough to satisfy the structural requirements for nanotechnology applications. Production and downstream processing should be aimed to maximizing assembled protein yields, and strategies for monitoring assembled protein structures during the production process need to be available. Traditional methodologies for protein purification and characterization are not sufficient to ensure the availability of required high amounts of correctly assembled macrostructures suitable for nanobiotechnology applications. Moreover, methodologies frequently used for the purification of viruses and virus-like particles have several disadvantages. High-speed preparative ultracentrifugation results in high shear forces and ionic strengths that can damage viral assemblies, provoke loss of their native activity, and result in materials with low purity that require additional purification steps, with consequent lower overall yields [11–13]. Additionally, ultracentrifugation is not practical at large scale, as it is time and labor consuming, expensive, and yields low recoveries. Chromatographic techniques are the alternative for purifying large quantities of the required multimeric materials [14]. In addition, integrative methodologies that maximize assembled protein recovery and allow the detailed characterization of the macromolecular assemblies are needed. A particular challenge is present when the insect cell–baculovirus expression system (IC–BEVS) is used for the production of multimeric proteins. Such an expression system is the most widely used for this kind of application, as it is versatile and highly productive. However, the presence of recombinant baculoviruses, which have a size and structure similar to that of recombinant nanotubes, impede the direct use of size-dependant purification steps.

In this work, down-stream processing strategies selective for VP6 tubular multimeric assemblies produced in the IC–BEVS were established along with process monitoring techniques. Purification steps were followed by dynamic light scattering (DLS), HPLC and ELISA in order to identify potential process bottlenecks. High-quality material, suitable for the synthesis of integrated hybrid nanobiomaterials, was obtained. The process designed here can be used for the production and characterization of other highly ordered macrostructures used as biological scaffolds for nanomaterials.

2. Materials and methods

2.1. Cell culture and recombinant protein production

High five insect cells (Invitrogen, Carlsbad, USA) were cultivated in SF900II medium (GIBCO-Invitrogen, Carlsbad, USA) in 1000 mL shaker flasks with 250 mL of working volume at 27 °C and 110 rpm. Exponentially growing cultures were resuspended in fresh medium to a viable cell density of 0.5×10^6 cell/mL and infected at a multiplicity of infection of 0.1 pfu/cell with a recombinant baculovirus (*Autographa californica* nucleopolyhedrovirus, AcMNPV) containing the rotavirus VP6 gene (strain SA11) under the very late *polh* promoter [15]. Baculovirus stocks were titrated using a cell viability assay [16]. Cell density and viability were monitored with a Coulter Counter (Coulter Electronics, Brea, USA) and by trypan blue exclusion, respectively.

2.2. SDS-PAGE, Western blot and ELISA

Protein samples were separated in a Laemmli SDS-PAGE system (12% resolving gels) stained with Coomassie blue. For immunodetection, proteins were transferred to nitrocellulose membranes (Millipore, Billerica, USA). Membranes were blocked with 5% low-fat dried milk in PBS for 30 min, incubated for 1 h with a rabbit anti-rotavirus polyclonal serum, washed three times with 0.1% low-fat milk in PBS and incubated with a secondary goat anti-rabbit antibody conjugated with peroxidase (Jackson Immunoresearch Labs, West Grove, USA) for 1 h. Peroxidase activity was detected by reaction with TMB (Invitrogen). VP6 concentration was measured with an ELISA kit (IDEIA Rotavirus, DakoCytomation (Cambridge, UK), later manufactured as ProSpecT, OXOID (Cambridge, UK), using a previously purified and characterized VP6 stock as standard.

2.3. Size distribution of viral multimeric assemblies

Size distribution of proteins was determined by size exclusion (SE) HPLC and DLS. HPLC analysis was performed as described by Mena et al. [17]. Briefly, a Waters (Milford, MA, USA) chromatographic system with an Ultrahydrogel 500 column was used in isocratic mode at a flow rate of 0.9 mL/min. The mobile phase was 10 mM Tris–HCl, 0.1 mM EDTA pH 8. Absorbance at 260 and 280 nm and fluorescence were monitored. The size exclusion column was calibrated with purified protein standards of lysozyme (hydrodynamic radius, R_H = 1.8 nm), trypsinogen (R_H = 2.2 nm), green fluorescence protein (R_H = 2.4 nm), ovoalbumin (R_H = 2.8 nm), bovine serum albumin (R_H = 3.5 nm), mouse immunoglobulin G (5.3 nm), and 30 nm standard fluorospheres (λ_{ex} = 505 nm, λ_{em} = 515 nm, Invitrogen). The column void volume (V_0) was determined with 100 nm standard fluorospheres and the total column volume (V_t) was determined with sodium azide. The partition coefficient (K_D) of each protein was calculated with the following equation:

$$K_D = \frac{V_e - V_0}{V_t - V_0}$$

where V_e is the elution volume of the protein peak.

Dynamic light scattering analysis was performed in a Zetasizer Nano ZS (Malvern, Worcestershire, UK) equipped with 4 mW He–Ne 633 nm laser with a detection angle of 173° backscatter at 25 °C in a low volume (45 μL) quartz suprasil cuvette (Hellma, Müllheim, Germany). Size distribution was obtained by intensity and volume measurements in multiple narrow mode. Measurements were performed at least in triplicate.

2.4. Transmission electron microscopy (TEM)

Micrographs were obtained in a transmission electron microscope (JEM1011, JEOL, Peabody, USA) operated at 80 kV. One drop of sample was put over a 200 mesh copper grid coated with formvar/carbon (ElectronMicroscopy Sciences, Washington, PA, USA), negatively stained by 3 min with 1% uranyl acetate and finally washed for 1 min with ultrapure water.

2.5. Purification of viral multimeric assemblies

2.5.1. Clarification and ultrafiltration

Infected cultures were harvested 96 h postinfection and clarified by centrifugation at 4000 × *g* for 10 min at 4 °C. The clarified supernatant was recovered and protease inhibitors were added (0.3 mg/mL of aprotinin and 1 mM of leupeptin). The supernatant and eluates of intermediate chromatographic steps were concentrated in an Amicon stirred ultrafiltration cell (Millipore, Billerica, USA) using a regenerated cellulose membrane of 30,000 NMWL, applying positive pressure (<55 psi). Alternatively, a hollow fiber cartridge of 650 cm^2 with a NMWL of 500,000 (A/G Technology Corporation) was used to concentrate culture supernatants before chromatographic processing.

2.5.2. Anion exchange chromatography (AEX)

An ÄKTAprime system (GE Healthcare, Waukesha, USA), with absorbance (280 nm), pH and conductivity on-line monitoring, was used. A XK-16 column (GE Healthcare) was packed with 40 mL of Q-Sepharose Fast Flow resin (GE Healthcare). The column was equilibrated with at least two column volumes of buffer A (Tris–HCl 30 mM, EDTA 0.1 mM, pH 6.16) at a flow rate of 2 mL/min. Prior to injection, the pH of the concentrated supernatant was adjusted to 6.16. Twenty milliliter of the concentrated supernatant were loaded, and the first peak, containing non-adsorbed components, was collected. Bound material was eluted with a 30 mM Tris–HCl, 0.1 mM EDTA, 1 M NaCl pH 6.16, and discarded.

2.5.3. Size exclusion chromatography (SEC)

Size exclusion chromatography was performed in a XK-26 column packed with 400 mL of Toyopearl HW65F resin (TOSOH Biosciences, San Francisco, USA). The column was equilibrated with at least two column volumes of buffer (Tris 30 mM, EDTA 0.1 mM, pH 8.0) at flow rate of 2.5 mL/min. The volume of concentrated sample loaded per run was 25 mL.

3. Results and discussion

The complete purification scheme developed in this work is described in Fig. 1 and step-by step recovery yields are listed in Table 1. Each step of the purification scheme was characterized, and is described below. The starting materials for purification were clarified culture supernatants, which had typical VP6 concentrations of 280 ± 30 mg/L (Table 1). Only $31 \pm 1\%$ of VP6 remained in the cellular pellet after clarification of the supernatant. A SDS-PAGE gel of the clarified culture supernatant showed that it was composed of proteins ranging from 120 to 20 kDa. Proteins with molecular weights similar to those of baculovirus gp64 and VP6 were the main components (data not shown). gp64 is the most abundant protein of the baculovirus envelope [18] and it indicates the presence of baculovirus particles. It was expected to find VP6 assembled into VP6 nanotubes in the clarified supernatant, as Mena et al. [19] demonstrated that VP6 nanotubes assemble intracelullarly.

The presence of VP6 nanotubes during the purification scheme was followed by SE-HPLC and DLS. Calibration curves for the HPLC system were constructed with the calibration standards listed in Section 2, injected at least three times each. Two linear standard curves were obtained, the first for K_D between 0 and 0.5, $R_H = 25.56(1 - K_D) - 9.99$ ($R^2 = 0.99$), and the second for K_D between 0.5 and 0.8, $R_H = 3.18(1 - K_D) + 1.13$ ($R^2 = 0.98$). Analysis of the clarified culture supernatant by SE-HPLC showed a peak with 2.8% of the total 280 nm absorbance that eluted with the void volume of the column, and thus it contained macrostructures with a $R_H > 15$ nm (peak 1, Fig. 2A). The macrostructures peak was expected to contain both VP6 nanotubes (70 nm in diameter and several micrometers in length [19]) and baculovirus particles (20 and 260 nm in diameter and length, respectively [18,20]). The 260/280 nm absorbance ratio of the macrostructure peak indicated that it contained 8% of nucleic acids (data not shown), suggesting the presence of baculovirus.

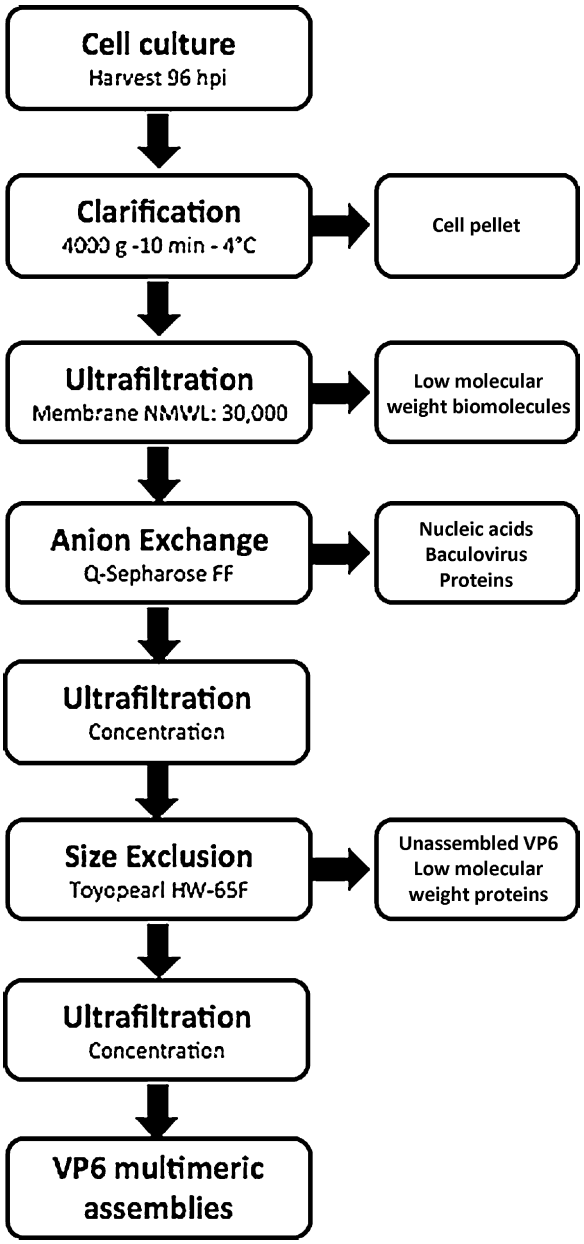

Fig. 1. Downstream purification steps for VP6 multimeric assemblies.

Other 4 peaks were detected in the SE-HPLC analysis. The second peak (mean R_H 7.7 nm) had 2.6% of the total 280 nm absorbance and did not absorb at 260 nm. The third peak had a protein content of 95%, a R_H between 6 and 2.5 nm, and 5% of nucleic acids. The fourth peak contained 30% of nucleic acids and proteins between 2.5 and 2 nm. The last peak (S) had a K_D close to 1 and corresponded to salts

Table 1
Yield of purification steps.

Purification step	Volume (mL)	VP6 concentration[a] (μg/mL)	VP6 step yield[b], (%)	VP6 overall yield[b] (%)
Clarified supernatant	500	281.4	–	100
Ultrafiltration	250	411.8	73.1	73.1
AEX	250	271.4	65.8	48.1
Ultrafiltration	100	531	82.9	39.8
SEC	180	265.2	85.0	33.9
Ultrafiltration	50	579.5	60.0	20.5

[a] As determined by ELISA in each step.
[b] Refers to VP6 recovery.

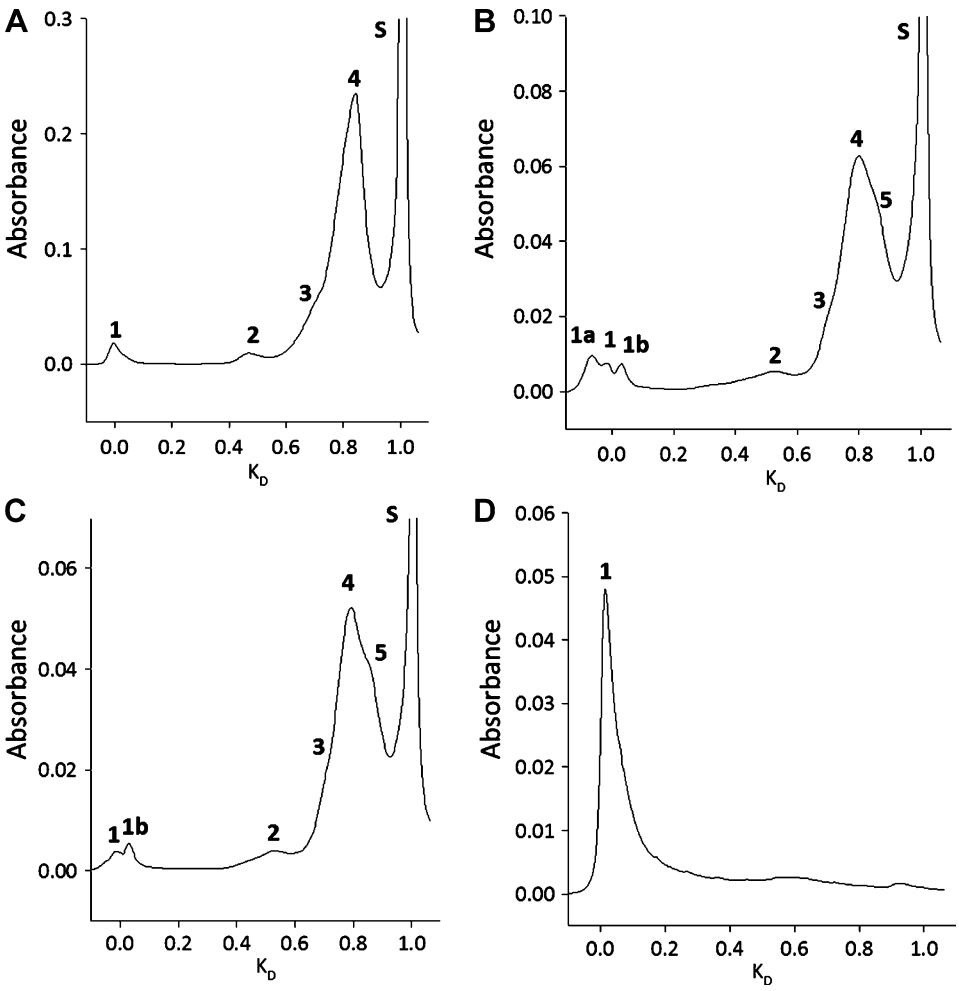

Fig. 2. Size exclusion (SE) HPLC analysis of purification steps: (A) culture supernatant; (B) concentrated supernatant; (C) peak 1 of AEX chromatography; (D) peak 1 of SEC.

present in the sample. Analysis by DLS showed that a typical culture supernatant contained particles with two size distributions, one with a mean R_H of 57 nm (73% of the volume, distribution *a*) and one of 170 nm (27% of the volume, distribution *b*) (Fig. 3A).

The next step for VP6 nanotube purification was the concentration of the clarified supernatant by ultrafiltration (Fig. 1). Two alternative configurations were tested: a hollow fiber cartridge with a NMWL of 500,000 or an Amicon stirred ultrafiltration cell. Only 55% of recombinant VP6 in the harvested supernatant was recovered after concentration in the hollow fiber cartridge, while 70% was recovered in the ultrafiltration cell. An additional advantage of the stirred cell is that it submits the nanotubes to a low shear, preventing damage of shear-sensitive viral assemblies [12]. Therefore, the ultrafiltration cell was chosen for VP6 concentration in the following steps of the purification scheme (Fig. 1).

The culture supernatant was initially concentrated to half its original volume. The presence of VP6 in the concentrated supernatant was confirmed by SDS-PAGE (image not shown). SE-HPLC analysis of the concentrated sample allowed the resolution of three peaks that eluted at a K_D close to 0, all containing macrostructures (peaks 1a, 1 and 1b, Fig. 2B). The peak in the center had a K_D similar to that of peak 1 in the non-concentrated supernatant. Peak 1a contained 15% of nucleic acids, while the other two contained less than 4%. This suggests that peak 1a corresponded to baculovirus particles, which contain viral DNA. The three macrostructure peaks had a relative abundance of 8.7%, three times more abundant than peak 1 in the non-concentrated clarified supernatant. Peak 1a had a relative abundance of 3.9% and constituted 44.8% of the macrostructures present in the concentrated sample. Populations corresponding to peaks 2, 3, and 4 of the chromatogram of the untreated clarified supernatant were also detected in the concentrated supernatant. An additional peak, labeled as 5, was detected as a shoulder of peak 4 in the concentrated sample. Peaks 1, 1b, 2 and 5 had a protein content above 95%. Nucleic acids were present mostly in peak 4, which contained 45% of the total 280 nm absorbance and 14% nucleic acids. In comparison, DLS of the concentrated supernatant showed three defined populations of particles with average diameters of 86, 323 and 1407 nm (Fig. 3B). The population with average diameter of 1407 nm was not observed in the DLS analysis of the non-concentrated culture supernatant. According to their size, all populations detected by DLS were expected to elute with peak 1 in SE-HPLC.

DLS analysis of the filtrate of the first ultrafiltration step showed only two populations, one with a mean diameter of 54 nm and the second of 323 nm (data not shown). No presence of the population with a mean diameter of 1407 nm (corresponding to the VP6 nanotubes) was observed in the filtrate. Analyses of the concentrated supernatant and filtrate show that VP6 nanotubes were not significantly removed from the sample during the ultrafiltration step. The loss of VP6 in the concentration step was possibly a result of the removal of unassembled VP6 (Table 1).

The next step in the purification scheme was anion exchange (AEX) chromatography, which is a common step used for the effective recovery, removal or inactivation of viruses in biotechnology products [20–23]. Fig. 4A shows a typical AEX chromatogram. The pH of the equilibration and elution buffers was adjusted to 6.16,

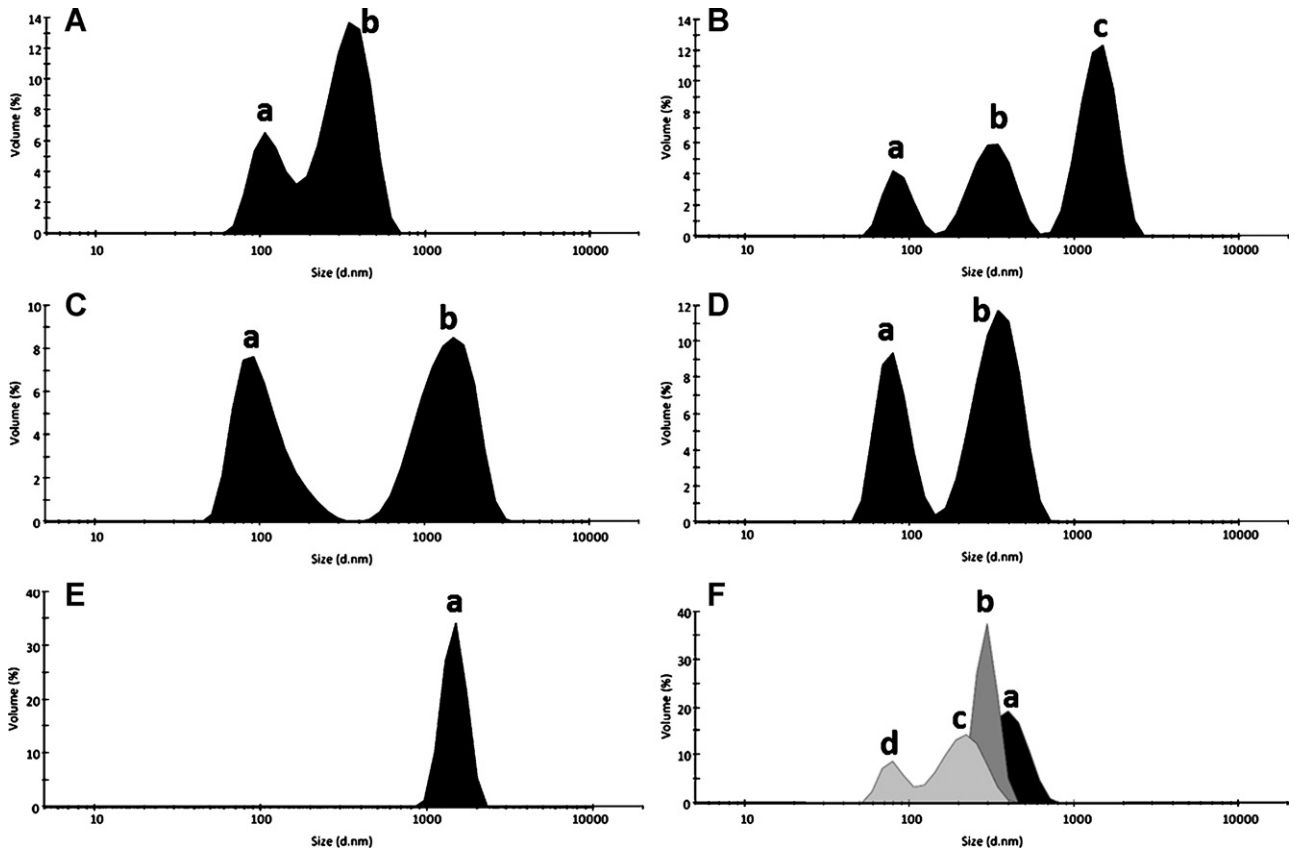

Fig. 3. Size distribution by volume of particles in the purification steps, as determined by DLS. The mean diameter of each population and their relative volume content are listed as follows: (A) Culture supernatant (population a: 115 nm, 27%; population b: 349 nm, 73%); (B) concentrated supernatant (population a: 86 nm, 14.6%; population b: 324 nm, 30.5%; population c: 1407 nm, 54.8%); (C) peak 1 of AEX chromatography (population a: 107.7 nm, 43%; population b: 1406 nm, 57%); (D) peak 2 of AEX chromatography (population a: 80.2 nm, 36.8%; population b: 348 nm, 63.2%); (E) first peak eluted from the SEC column (population a: 1461 nm, 100%); (F) other peaks eluted from the SEC column; black, peak 2 (population a: 387 nm, 100%); dark gray, peak 3 (population b: 295 nm, 100%); light gray, peak 4 (population c: 212 nm, 73.2%; population d: 80.2 nm, 26.8%).

the calculated isoelectric point of VP6, because under these conditions it was expected that nucleic acids and baculovirus gp64 interacted with the resin and remained adsorbed, while VP6 tubes flowed through. Accordingly, SDS-PAGE of peaks 1 and 2 of the AEX chromatography showed that gp64 was absent in peak 1 and abundant in peak 2, and that most VP6 did not bind to the column. AEX resins have been used to bind viruses (X-MuLV, MMV and SV40) and gp64 through electrostatic interactions [20–22,24]. The recovery yield of the AEX step was 65.8%, and the overall yield was 48.1% to this step (Table 1).

Peak 1 of AEX was analyzed by SE-HPLC (Fig. 2C). Peak 1a, present in the concentrated supernatant, was removed by AEX. This, and the absence of gp64 in peak 1 (as determined by SDS-PAGE), evidenced that baculovirus particles were eliminated by AEX. Macrostructures present in peak 1 of AEX eluted in peaks 1 and 1b of SE-HPLC, which corresponded to 4.2% of the total absorbance at 280 nm (Fig. 2C). This relative abundance was similar to that observed in the concentrated supernatant. Peaks 2, 3, 4 and 5 found in the sample of the concentrated supernatant were also observed in peak 1 of AEX, with a similar relative abundance. Analysis by DLS of peak 1 of AEX showed only two populations (a and b) with mean diameters of 108 and 1406 nm, which corresponded to 43% and 57% of the size distribution by volume, respectively (Fig. 3C). Population b had a size distribution similar to that of population c in the concentrated supernatant (Fig. 3B). The second AEX peak, which contains materials adsorbed to the column, contained also two populations but with different sizes (Fig. 3D). The first population had a mean diameter of 80 nm and represented 37% of volume, and the second population, corresponding to 63% of the total volume, had a mean diameter of 348 nm. The particle size of the largest population is characteristic of baculovirus particles, which have 300–400 nm in length [20]. SDS-PAGE, SE-HPLC and DLS showed that the AEX step was effective for complete removal of baculovirus particles, the main contaminant in the supernatant, represented by gp64 in SDS-PAGE (image not shown). The first peak of AEX was concentrated by ultrafiltration, where 83% of the VP6 was recovered (Table 1).

In absence of baculovirus particles, size exclusion chromatography (SEC) is the best option to selectively purify assembled VP6 nanotubes, which should be the only macrostructure remaining. Thus, this was the next process in the design purification scheme (Fig. 1). The Toyopearl HW65F resin was selected for this step (average pore diameter of 100 nm). The first peak of SEC contained only highly pure (>98%) VP6 nanotubes and eluted after 150 ml of sample injection (Fig. 4B). Three additional peaks were observed. VP6 was detected in minor amounts in peaks 2 and 3. SEC VP6 recovery yield was 85% and the total yield to this step was 33.9%. DLS analysis revealed that peak 1 contained a single population ranging from 900 to 2500 nm with a mean hydrodynamic diameter of 1460 nm (Fig. 3E), whereas peaks 2, 3 and 4 contained proteins distributed in populations between 387 and 80 nm in diameter (Fig. 3F).

Peak 1 of SEC, containing VP6 nanotubes, was concentrated by ultrafiltration and further analyzed. The final concentration step had a yield of 60%, lower to that observed in previous ultrafiltration steps (Table 1). This low yield could be a result of binding of

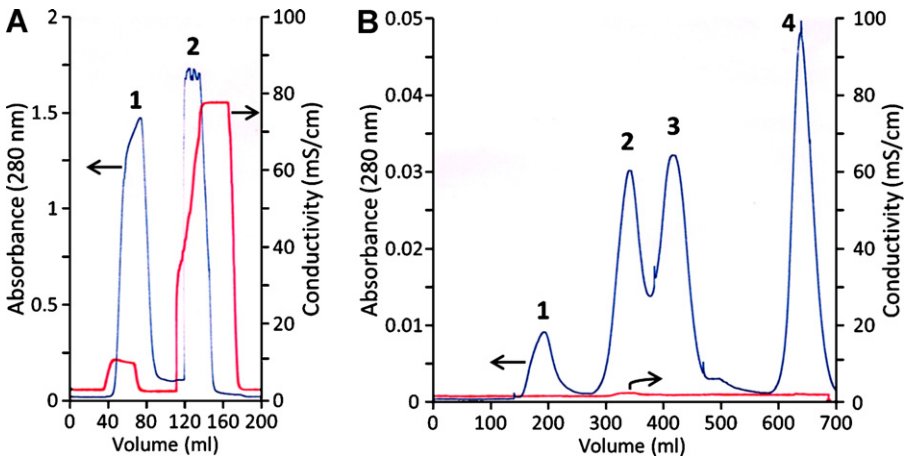

Fig. 4. Chromatograms of the chromatography purification steps: (A) anion exchange; (B) size exclusion chromatography. Absorbance (280 nm) and conductivity (mS/cm), as indicated by the arrows, are shown.

the VP6 nanotubes to the ultrafiltration cellulose membrane. SE-HPLC showed a single peak with a K_D close to 0 (Fig. 2D). Such a peak had a protein content higher than 95%, as calculated from the 260/280 absorbance ratio. SDS-PAGE analysis of the concentrated sample showed a single band with a molecular weight of 45 kDa, which corresponds to the molecular weight of VP6. No contaminant proteins were detected in the gel. The identity of the band was confirmed as VP6 by Western blot, where a single band of 45 kDa was detected. No product of degradation of VP6 was observed. The presence and morphology of VP6 assembled into nanotubes was confirmed by TEM (Fig. 5). Nanotubes with a diameter of 75 nm and various micrometers in length were observed, confirming the size distribution determined by DLS. Their structural characteristics were similar to those previously reported by Lepault et al. [8] and Plascencia-Villa et al. [10]. The surface lattice of VP6 nanotubes had a regular hexagonal pattern with the negative stain accumulated in the center of trimers and along the edges, revealing the structural consistency of the viral multimeric structures obtained (Fig. 5). The viral multimeric assemblies of VP6 purified with the downstream process described here were only nanotubes with a mean length of 1460 nm, assuming a spherical particle shape. Their size was monodisperse and ranged between 900 and 2500 nm (Fig. 3E). In comparison with TMV and M13 bacteriophage, which are viral assemblies commonly used as biotemplates, VP6 nanotubes were over four- and two-fold longer, respectively [25,26].

The purification scheme designed in this work is summarized in Table 1 and Fig. 1. The overall yield of the purification process was 20.5%, which is low compared with purification schemes designed for individual proteins. It must be considered that only assembled VP6 was recovered. In comparison with traditional purification schemes for viral assemblies, the obtained recovery yield was 4.7 times higher than the best yields reported for ultracentrifugation schemes (1.6–4.4%) [11,13]. Furthermore, purity was increased from 9% in ultracentrifugation schemes to over 95% obtained in this work. The scheme presented here is suitable for scale-up and useful for reproducible purification at large-scale of viral multimeric structures, with a low cost and in a short process time. Moreover, the same purification scheme can be implemented to purify other viral multimeric structures produced in the IC–BEVS with minor adjustments. For example, double-layered rotavirus-like particles with 75 nm in diameter have been purified in our laboratory following the same scheme, obtaining as a product only the desired particles. The obtained VP6 nanotubes were suitable for functionalization with metals and the production of hybrid nanomaterials, as described in Plascencia-Villa et al. [10].

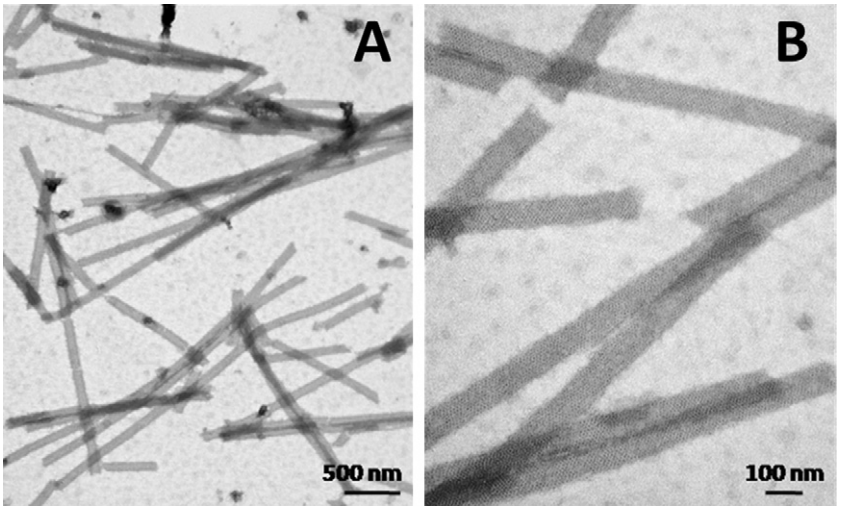

Fig. 5. Characterization by TEM of purified VP6 nanotubes: (A) 30,000×; (B) 100,000×. The samples were negatively stained with uranyl acetate.

4. Conclusions

The development of downstream bioprocesses to obtain viral macrostructures with high compositional and structural uniformity, with high yields, in short time and with reduced cost is a challenge that must be solved for the efficient use of viral macrostructures in several fields. The IC–BEVS offers the advantage of producing correctly assembled viral multimeric proteins with high yields. However, it has the disadvantage of the presence of the baculovirus vector as byproduct. The downstream purification strategy implemented here was able to process large volumes with high yields (20.5%), in comparison with traditional time-consuming schemes. The process has a low cost and can be easily scaled-up, in contrast to traditional ultracentrifugation schemes. The final quality and purity was >98% of only correctly assembled VP6 nanotubes. The structure of the viral multimeric protein was preserved, as confirmed by SE-HPLC and DLS analysis during the purification steps and by TEM of the final product. SE-HPLC and DLS provided complementary information that aided in down-stream process design, monitoring and quantification. SE-HPLC allowed the detection of small size structures, while DLS provided information about the size distribution of macrostructures present in samples. DLS provides information of size distributions in heterogeneous samples in short time, which allows immediate process monitoring necessary for taking opportune decisions.

The purification scheme presented here produced high quality nanotubes suitable for functionalization with metals, as described previously [10]. Viral multimeric assemblies formed by rotavirus VP6 are multifunctional versatile scaffolds for the *in situ* synthesis of noble metal, magnetic and semiconductor nanoparticles that remain conjugated over the reactive amino acid residues to produce integral hybrid nanobiomaterials with high morphological consistency and multiple applications in material sciences and potential uses in nanomedicine.

Acknowledgements

Financial support by CONACyT-Salud (2007-C01-69911), SEP-CONACyT 2008-01-101847 and PAPIIT-UNAM 224409. Funding agencies had no involvement in study design or in the collection, analysis or interpretation of data. GPV, RCA and JCF are grateful for the support of CONACyT during their graduate studies. JAM was supported during his graduate studies by DGEP-UNAM. Technical support is provided by Ana Ruth Pastor, Alba Lecona and Vanessa Hernández. Electron Microscopy Facilities are of the Instituto Nacional de Salud Pública, Mexico.

References

[1] E.R. Ballister, A.H. Lai, R.N. Zuckermann, Y. Cheng, J.D. Mougous, Proc. Natl. Acad. Sci. 105 (2008) 3733.
[2] S. Mann, Nat. Mater. 8 (2009) 781.
[3] T.J. Ueno, J. Mater. Chem. 18 (2008) 3741.
[4] S. Zhang, Nat. Biotechnol. 21 (2003) 1171.
[5] T. Douglas, M. Young, Science 312 (2006) 873.
[6] M. Fischlechner, E. Donath, Angew. Chem. Int. Ed. 46 (2007) 3184.
[7] P. Singh, M.J. Gonzalez, M. Manchester, Drug. Dev. Res. 67 (2006) 23.
[8] J. Lepault, I. Petitpas, I. Erk, J. Navaza, D. Bigot, M. Dona, P. Vachette, J. Cohen, F.A. Rey, EMBO J. 20 (2001) 1498.
[9] J.A. Mena, R.M. Castro-Acosta, O.T. Ramírez, L.A. Palomares, Assembly kinetics of rotavirus VP6: from nanotubes to icosahedral structures, submitted for publication.
[10] G. Plascencia-Villa, J.M. Saniger, J.A. Ascencio, L.A. Palomares, O.T. Ramírez, Biotechnol. Bioeng. 104 (2009) 871.
[11] J. Benavides, J.A. Mena, M. Cisneros, O.T. Ramírez, L.A. Palomares, M. Rito-Palomares, J. Chromatogr. B 842 (2006) 48.
[12] R. Morenweiser, Gene. Ther. 12 (2005) S103.
[13] L. Pedro, S.S. Soares, G.N.M. Ferreira, Chem. Eng. Technol. 31 (2008) 815.
[14] L.K. Pattenden, A.P.J. Middelberg, M. Niebert, D.I. Lipin, Trends. Biotechnol. 23 (2005) 523.
[15] L.A. Palomares, S. López, O.T. Ramírez, Biotechnol. Bioeng. 78 (2002) 635.
[16] J.A. Mena, O.T. Ramírez, L.A. Palomares, BioTechniques 34 (2003) 260.
[17] J.A. Mena, O.T. Ramírez, L.A. Palomares, J. Chromatogr. B 824 (2005) 267.
[18] L.A. Palomares, S. Estrada-Mondaca, O.T. Ramírez, in: S. Ozturk, W.S. Hu (Eds.), Cell Culture Technology for Pharmaceutical and Cellular Applications, CRC Press, New York, 2006, p. 627.
[19] J.A. Mena, O.T. Ramírez, L.A. Palomares, J. Biotechnol. 122 (2006) 443.
[20] T. Vicente, C. Peixoto, M.J.T. Carrondo, P.M. Alves, Gene. Ther. 16 (2009) 766.
[21] D.M. Strauss, J. Gorrell, M. Plancarte, G.S. Blank, Q. Chen, B. Yang, Biotechnol. Bioeng. 102 (2009) 168.
[22] D.M. Strauss, S. Lute, Z. Tebaykina, D.D. Frey, C. Ho, G.S. Blank, K. Brorson, Q. Chen, B. Yang, Biotechnol. Bioeng. 104 (2009) 371.
[23] T. Vicente, M.F.Q. Sousa, C. Peixoto, J.P.B. Mota, P.M. Alves, M.J.T. Carrondo, J. Membr. Sci. 311 (2008) 270.
[24] J. Kadlec, S. Loureiro, N.G. Abrescia, D.I. Stuart, I.M. Jones, Nat. Struct. Mol. Biol. 15 (2008) 1024.
[25] E. Dujardin, C. Peet, G. Stubbs, J.N. Culver, S. Mann, Nano Lett. 3 (2003) 413.
[26] K.T. Nam, R. Wartena, P.J. Yoo, F.W. Liau, Y.J. Lee, Y.M. Chiang, P.T. Hammond, A.M. Belcher, Proc. Natl. Acad. Sci. 105 (2008) 17227.